Finite-Difference Approach to Scattering of Sound Waves in Fluids

R.T. Ling*
Northrop Aircraft Division, Hawthorne, California

The finite-difference approach based on the concept of the generalized scattering amplitude is extended to sound scatterings by three-dimensional obstacles. Numerical results for an example problem of scattering by a sphere are obtained for $ka=5$, where k is the wave number equaling 2π divided by the wavelength of the sound waves and a is the radius of the sphere. These results are in excellent agreement with those obtained by the eigenfunction expansion method. Results presented include spatial profiles of the generalized scattering amplitude, amplitude and phase of the total sound pressure, and bistatic scattering cross sections. The method shows promise for accurate, systematic calculations for bodies of arbitrary material, size, and shape. It is also applicable to classical scattering of electromagnetic waves and quantum scattering of particles.

I. Introduction

RECENTLY, a finite-difference approach[1,2] to scattering problems has been successfully applied to scalar scatterings of sound waves by long circular cylinders and vector scatterings of electromagnetic waves by perfectly conducting spheres. This approach employs the concept of the radially nonoscillatory generalized scattering amplitude to circumvent the numerical difficulty due to the oscillatory behavior of field quantities in the infinite exterior region. A similar concept called wave envelope[3] was used in various studies of sound propagation in ducts. In this paper, we extend the finite-difference approach to sound scatterings by three-dimensional obstacles using the sphere as an example. Both acoustically soft and hard spheres are considered.

II. Differential Equation Formulation for the Generalized Scattering Amplitude

The problem under consideration is that of a plane wave of sound incident on an obstacle immersed in a fluid medium through which the sound waves propagate. The problem can be formulated in any arbitrary coordinate system such as a numerically generated curvilinear coordinate system for a complex geometry obstacle. The schematics of the sound scattering by a sphere and spherical coordinate system are illustated in Fig. 1 as an example. The incident sound wave of wavelength λ and frequency ν propagates in the positive z axis direction and is represented by $\exp[i(kz-wt)]$, where $k=2\pi/\lambda$ is the wave number and $w=2\pi\nu$ is the angular frequency. The sphere's radius is denoted by a.

The theory described in Ref. 1 can be readily generalized to the scattering of sound waves by a sphere. The major change involves the generalized scattering amplitude, which is now modulated by an outgoing three-dimensional spherical wave e^{ikr}/kr with $r=\sqrt{x^2+y^2+z^2}$ being the radius vector from the coordinate origin. This compares with an outgoing two-dimensional cylindrical wave $e^{ikr}/\sqrt{kr}$ that modulates the two-dimensional generalized scattering amplitude where $r=\sqrt{x^2+y^2}$ is the position vector in the two-dimensional polar coordinate plane. The difference in modulating waves results in a slightly different form of radiation condition for three-dimensional sound scatterings:

$$\lim_{r\to\infty} r\left(\frac{\partial}{\partial r}-ik\right)\psi^s=0 \tag{1}$$

where ψ^s is the scattered wave.

If the incident sound wave propagates along the z axis, the spherical symmetry of the obstacle and the longitudinal nature of sound waves make the sphere scattering problem independent of the azimuthal angle ϕ. Thus, the total wave ψ can be written as

$$\psi=e^{ikz}+f(r,\theta)\frac{e^{ikr}}{kr} \tag{2}$$

where $f(r,\theta)$ is the generalized scattering amplitude. Substitution of Eq. (2) in the three-dimensional Helmholtz equation results in a transformed Helmholtz equation

$$\frac{\partial^2 f}{\partial r^2}+2ik\frac{\partial f}{\partial r}+\frac{\cot\theta}{r^2}\left(\frac{\partial f}{\partial\theta}\right)+\frac{1}{r^2}\frac{\partial^2 f}{\partial\theta^2}=0 \tag{3}$$

for the generalized scattering amplitude in spherical coordinates.

In terms of the generalized scattering amplitude, the radiation conditions and surface boundary condition can be written in exactly the same form as Eqs. (8) and (9) in Ref. 1. The three-dimensional bistatic cross section is defined as

$$\sigma(\theta,\phi)=\lim_{r\to\infty} 4\pi r^2\frac{|\psi^s|^2}{|\psi^i|^2} \tag{4}$$

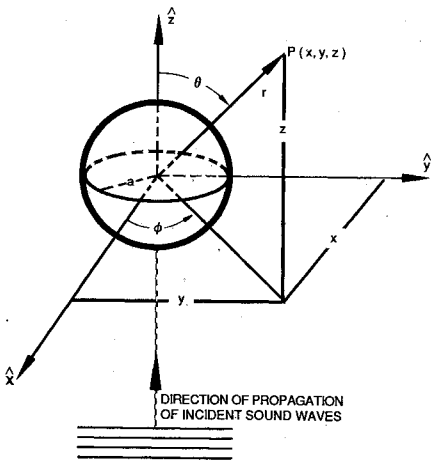

Fig. 1 Plane wave incidence on a sphere and the coordinate systems.

Received Jan. 13, 1987; revision received May 28, 1987.

*Engineering Specialist. Member AIAA.

where ψ^i is the incident plane wave. For the unit amplitude plane wave e^{ikz} in Eq. (2), it follows that

$$\sigma(\theta,\phi)=\frac{4\pi}{k^2}|f(\infty,\theta)|^2 \tag{5}$$

The total acoustic scattering cross section σ_T is given by

$$\sigma_T=\frac{1}{4\pi}\int_0^{\pi}d\theta\int_0^{2\pi}d\phi\sigma(\theta,\phi)\sin\theta$$

$$=\frac{2\pi}{k^2}\int_0^{\pi}|f(\infty,\theta)|^2\sin\theta d\theta \tag{6}$$

and the optical theorem becomes

$$\sigma_T=\frac{4\pi}{k^2}f^i(\infty,0) \tag{7}$$

where $f^{(i)}$ $(\infty,0)$ is the imaginary part of the asymptotic scattering amplitude in the forward direction.

III. Finite-Difference Technique

The finite-difference techniques described in Ref. 1 can be employed to solve Eq. (3). The physical space (Fig. 2) is mapped into the computational space (Fig. 3) for the numerical solution of Eq. (3). For sound scatterings by a sphere, a slight complication occurs in the evaluation of the $\cot\theta\partial f/\partial\theta$ term in the equation at $\theta=0$ and π. Due to the symmetry property of the equation and boundary conditions under the transformation $\theta\rightarrow-\theta$, one has $f(r,\theta)=f(r,-\theta)$ for all r and θ. It follows that $\partial f/\partial\theta=0$ at $\theta=0$ and π. The $\cot\theta\partial f/\partial\theta$ term appears to have an indefinite value at these two angles. However, by making the coordinate transformation $\mu=\cos\theta$, it can be shown that $\cot\theta\ (\partial f/\partial\theta)=(\partial^2 f/\partial\theta^2)-(\partial^2 f/\partial\mu^2)(1-\mu^2)$ for all θ values. Since $\mu^2=1$ and $\partial^2 f/\partial\mu^2$ is finite at $\theta=0$ and π, one obtains $\cot\theta\ (\partial f/\partial\theta)=(\partial^2 f/\partial\theta^2)$ at these two angles. Therefore, the transformed Helmholtz equation assumes the form

$$\frac{\partial^2 f}{\partial r^2}+2ik\frac{\partial f}{\partial r}+\frac{2}{r^2}\frac{\partial^2 f}{\partial\theta^2}=0 \tag{8}$$

at $\theta=0$ and π.

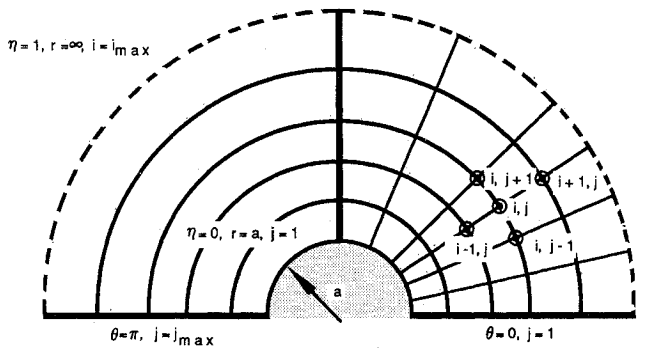

Fig. 2 Physical space.

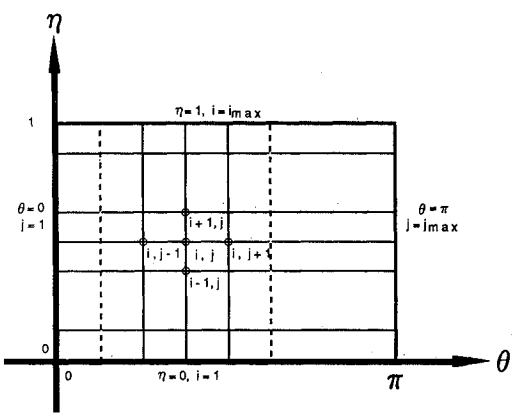

Fig. 3 Computational space.

IV. Numerical Results and Discussion

For a plane sound wave incident on a sphere, the eigenfunction expansion method has been used by Bowman et al.[4] to compute the amplitude and phase of the scattered waves for various ka values. Morse[5] provided the intensity of the scattered wave at $ka=1$, 3, and 5 for scattering by a rigid (hard) sphere. In this section, we present solutions based on the approach outlined in Secs. II and III and compare them with the results from the eigenfunction expansion method.

A. Soft-Sphere Scattering

For scattering by an acoustically soft sphere at $ka=5$, profiles of the generalized scattering amplitude are shown in Figs. 4-6 for scatterings in the forward, perpendicular, and

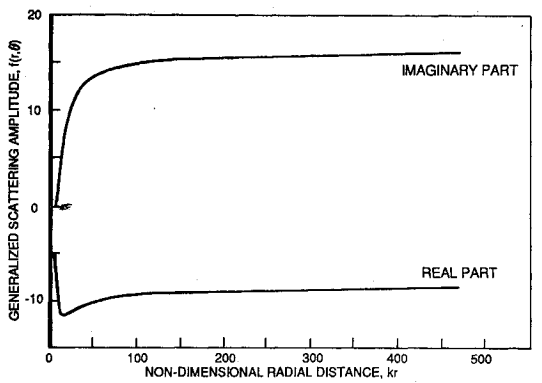

Fig. 4 Generalized scattering amplitude profiles; soft sphere, $ka=5$, $\theta=0$.

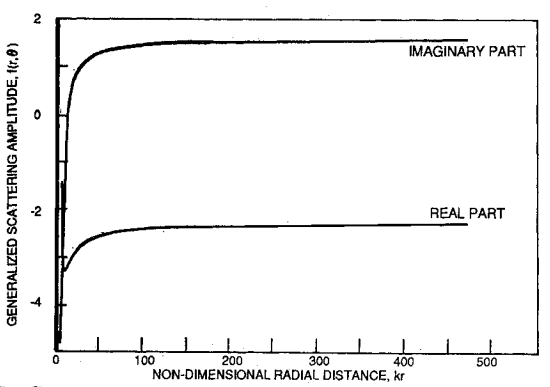

Fig. 5 Generalized scattering amplitude profiles; soft sphere, $ka=5$, $\theta=\pi/2$.

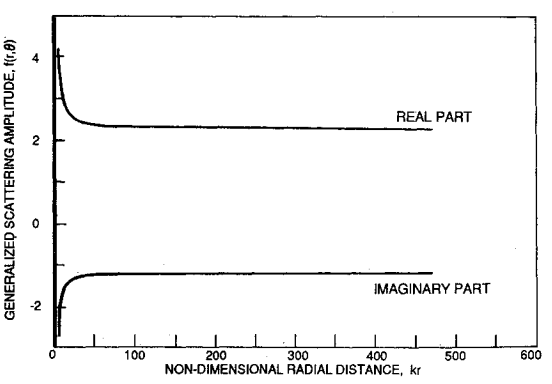

Fig. 6 Generalized scattering amplitude profiles; soft sphere, $ka=5$, $\theta=\pi$.

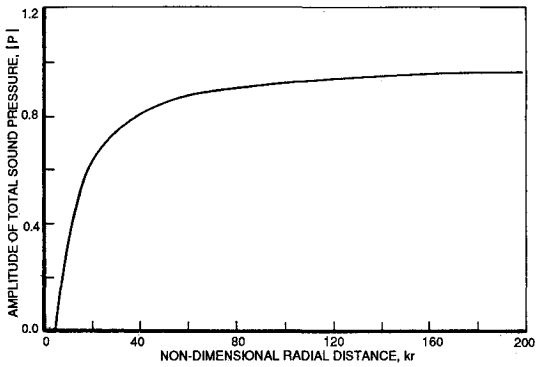

Fig. 7 Amplitude of total sound pressure; soft sphere, $ka=5$, $\theta=0$.

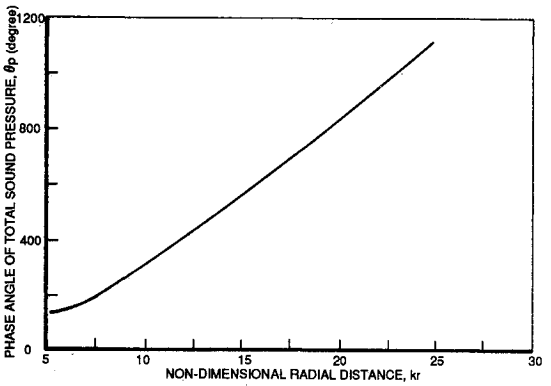

Fig. 8 Phase of total sound pressure; soft sphere, $ka=5$, $\theta=0$.

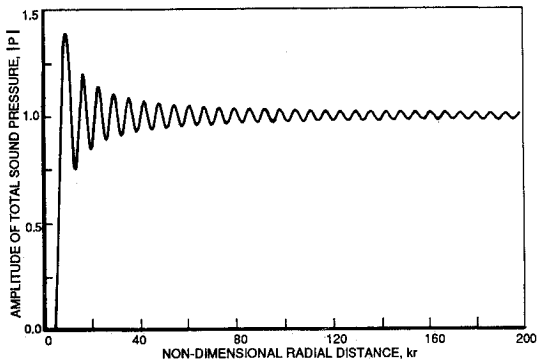

Fig. 9 Amplitude of total sound pressure; soft sphere, $ka=5$, $\theta=\pi/2$.

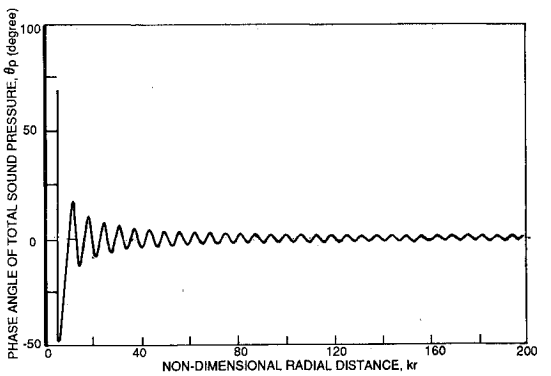

Fig. 10 Phase of total sound pressure; soft sphere, $ka=5$, $\theta=\pi/2$.

backscattering directions. As in the circular cylinder scattering case, there exists a strong interaction region with large gradients in the generalized scattering amplitude near the sphere's surface. Figures 7–12 show the amplitude and phase of the

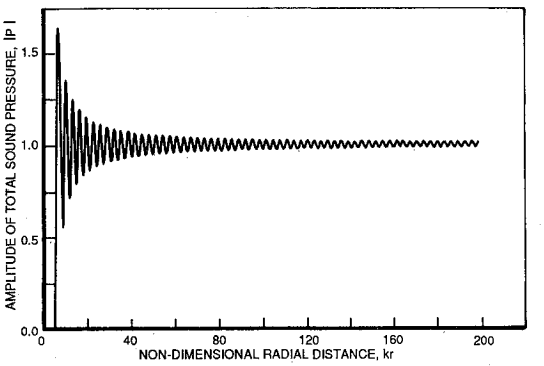

Fig. 11 Amplitude of total sound pressure; soft sphere, $ka=5$, $\theta=\pi$.

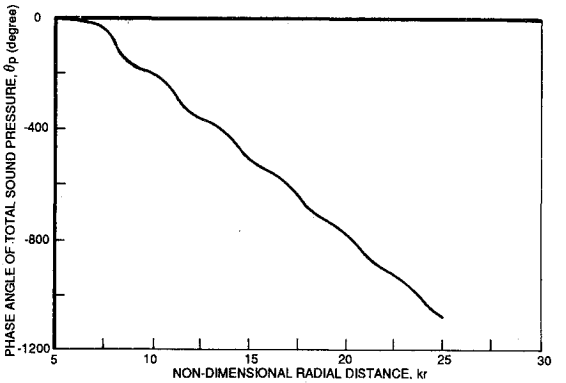

Fig. 12 Phase of total sound pressure; soft sphere, $ka=5$, $\theta=\pi$.

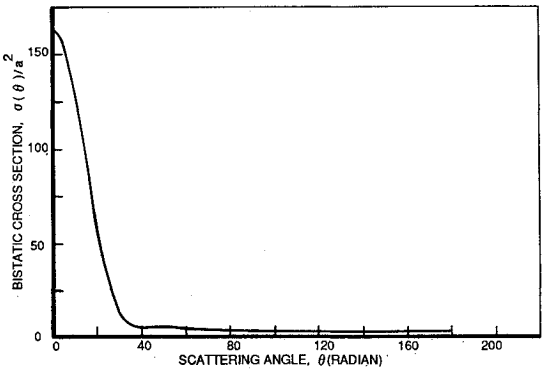

Fig. 13 Distribution of bistatic cross sections; soft sphere, $ka=5$.

total sound pressure computed from Eq. (2). The amplitudes of the total waves are normalized to the incident wave amplitude, which is taken to be unity. The behavior of the total wave can be explained as a result of the interference between the incident wave and the scattered wave.

The interference effect can be seen explicitly from the simple expressions for the amplitude of the total wave in the forward, perpendicular, and backscattering directions. These expressions can be obtained by replacing $\sqrt{kr}$ with kr and by replacing kr with k^2r^2 in the corresponding equations in Ref. 1. Figure 13 shows the bistatic cross section in units of a^2 as a function of scattering angle for a soft sphere at $ka=5$. The scattered wave intensity in the far field peaks in the forward direction. Figure 14 shows the amplitude of the induced "surface current" defined by

$$J(\theta)=\frac{1}{k}\left(\frac{\partial\psi}{\partial r}\right)_{r=a}$$

analogous to that in electromagnetic wave scattering. These results are in excellent agreement with those of the eigenfunction expansion method given in Ref. 4. They are indistinguishable within graph accuracies from each other.

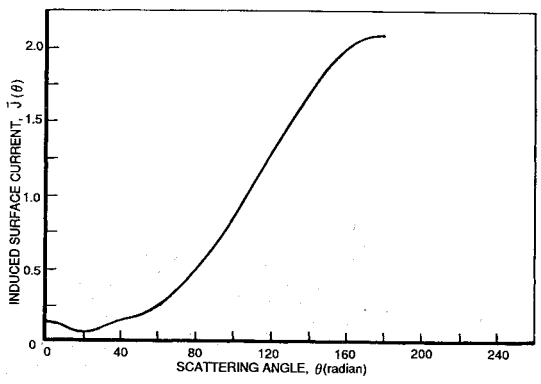

Fig. 14 Distribution of induced surface current; soft sphere, $ka=5$.

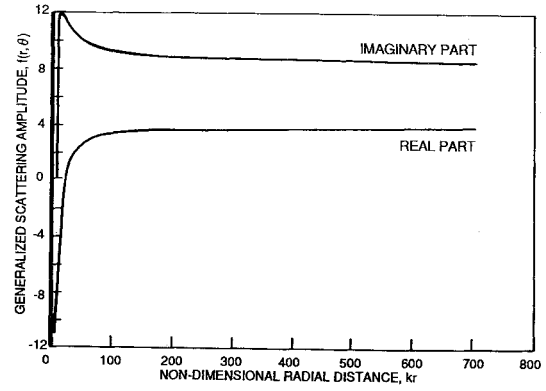

Fig. 15 Generalized scattering amplitude profile; hard sphere, $ka=5$, $\theta=0$.

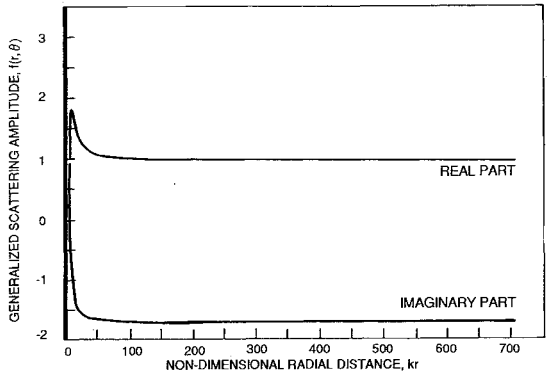

Fig. 16 Generalized scattering amplitude profile; hard sphere, $ka=5$, $\theta=\pi/2$.

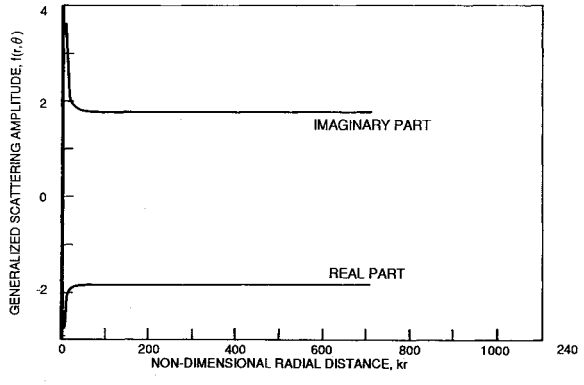

Fig. 17 Generalized scattering amplitude profile; hard sphere, $ka=5$, $\theta=\pi$.

As a further check on the accuracy and consistency of the numerical results presented so far, we use the optical theorem, which relates the total scattering cross section to the forward scattering amplitude. The total scattering cross section obtained from integating the bistatic cross sections is $8.162a^2$ for a soft sphere. This is in excellent agreement with the data shown in Ref. 4. The total scattering cross section computed from the imaginary part of the forward scattering amplitude is $8.032a^2$. The optical theorem is satisfied to within 2% error.

The problem of classical sound wave scattering by an "acoustically soft" sphere discussed here is mathematically equivalent to that of quantum mechanical scattering of a particle by a "hard" sphere. A quantum mechanically hard sphere is characterized by a repulsive three-dimensional spherical potential barrier of infinite height inside which the incident particle cannot penetrate and the wave function vanishes. This is exactly the boundary condition for the sound pressure at the surface of an acoustically soft sphere. Outside the hard sphere, the incident particle behaves as a free particle. Because the time-independent Schroedinger equation for the incident particle outside the hard sphere reduces to the Helmholtz equation, the governing equation is the same in both cases. The far-field condition for quantum scattering is usually written in the asymptotic form

$$\lim_{r\to\infty} \psi \to e^{ikz} + f(\infty,\theta)\frac{e^{ikr}}{kr} \tag{9}$$

where the ordinary scattering amplitude $f(\infty,\theta)$ is a function of scattering angle only. This asymptotic form of the wave function is equivalent to the radiation condition for the generalized scattering amplitude. As a consequence, the numerical results presented can be interpreted as those for the quantum scattering of a particle by a hard sphere. The wave number k has its usual meaning in quantum mechanics, with λ now being the de Broglie wavelength of the incident particle. The only additional consideration in the correspondence is that the quantum differential scatter cross sections are defined without the 4π factor in Eq. (4), which defines the acoustic bistatic cross sections. Because the total quantum scattering cross section is defined as the sum (instead of the average) of differential cross sections over the scattering angles, the numerical values for the total cross section in both cases are identical.

B. Hard-Sphere Scattering

For scattering by an acoustically hard sphere at $ka=5$, the profiles of the generalized scattering amplitude at scattering angles $\theta=0$, $\pi/2$, and π are shown in Figs. 15–17. As in the soft-sphere scattering case, these profiles show the existence of a strong interaction region characterized by large gradients in the generalized scattering amplitude near the sphere's surface. The profile of the bistatic cross sections in units of a^2 is shown in Fig. 18. The scattered wave intensity in the far field also peaks in the forward direction. The distribution of induced surface current $J(\theta)=|\psi(a,\theta)|$ on the hard sphere's surface is shown in Fig. 19. These results are in excellent agreement with eigenfunction expansion solutions given in Ref. 4.

The soft and hard sphere computations were performed separately due to the different surface boundary conditions. Typical CPU time for the computation of the complete scattered field with a 77×33 grid network is less than one minute on an IBM 3081 machine.

V. Conclusions

The presented results demonstrate that the finite-difference method for the solution of the transformed Helmholtz equation is an accurate and efficient numerical method for the scattering of sound waves. The basic feature of this approach is the introduction of the nonoscillatory generalized scattering amplitude, which characterizes the scattering problems. This

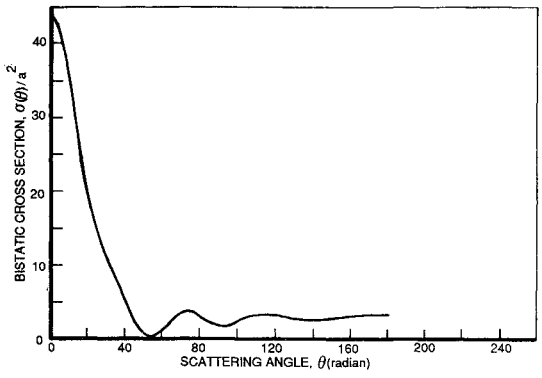

Fig. 18 Distribuion of bistatic cross sections; hard sphere, $ka = 5$.

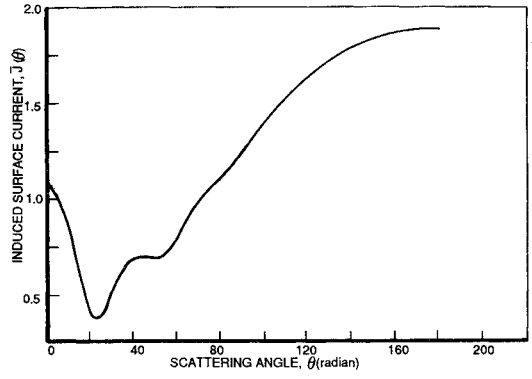

Fig. 19 Distribution of induced surface current; hard sphere, $ka = 5$.

introduction makes it possible to apply the finite-difference method to scattering problems in a manner similar to the application of this method to numerical solutions of ordinary fluid dynamics problems. The flexibility of the finite-difference method allows ready generalization for application to complex body shapes, size, and material properties of the scattering obstacle.

Acknowledgments

The author expresses his appreciation to Mr. M. W. George and Mr. H. A. Gerhardt for managerial support of this study. This work was performed under Northrop's Independent Research and Development Program.

References

[1]Ling, R.T., "Numerical Solution for the Scattering of Sound Waves by a Circular Cylinder," *AIAA Journal*, Vol. 25, April 1987, pp. 560–566.

[2]Ling, R.T., "Application of Computational Fluid Dynamics (CFD) Methods to Numerical Study of Electromagnetic Wave Scattering Phenomena," AIAA Paper 87-0487, Jan. 1987.

[3]Baumeister, K.J., "Finite-Difference Theory for Sound Propagation in a Lined Duct with Uniform Flow Using the Wave Envelope Concept," NASA TP 1001, 1977.

[4]Bowman, J.J., Senior, T.B.A., and Uslenghi, P.L.E., *Electromagnetic and Acoustic Scattering by Simple Shapes*, North-Holland, Amsterdam, 1969.

[5]Morse, P.M., *Vibration and Sound*, McGraw-Hill, New York, 1948.